Published in "Physics Procedia 17: 159-167, 2011"
which should be cited to refer to this work.

The search for the neutron electric dipole moment at the Paul Scherrer Institute

C. A. Baker[a], G. Ban[b], K. Bodek[c], M. Burghoff[d], Z. Chowdhuri[e], M. Daum[f,e,g], M. Fertl[e,h], B. Franke[f,e], P. Geltenbort[i], K. Green[a,j], M. G. D. van der Grinten[a,j], E. Gutsmiedl[k], P. G. Harris[j], R. Henneck[e], P. Iaydjiev[a,1], S. N. Ivanov[a,2], N. Khomutov[l], M. Kasprzak[m], K. Kirch[e,h], S. Kistryn[c], S. Knappe-Grüneberg[d], A. Knecht[e,3], P. Knowles[m], A. Kozela[n], B. Lauss[e], T. Lefort[b], Y. Lemière[b], O. Naviliat-Cuncic[b,o], J. M. Pendlebury[j], E. Pierre[b,e], F. M. Piegsa[h], G. Pignol[p], G. Quéméner[b], S. Roccia[q,4], P. Schmidt-Wellenburg[e], D. Shiers[j], K. F. Smith[j], A. Schnabel[d], L. Trahms[d], A. Weis[m], J. Zejma[c], J. Zenner[e,r], G. Zsigmond[e]

[a] *Rutherford Appleton Laboratory, Chilton, Didcot, Oxon OX11 0QX, United Kingdom*
[b] *LPC Caen, ENSICAEN, Université de Caen, CNRS/IN2P3, F–14050 Caen, France*
[c] *Marian Smoluchowski Institute of Physics, Jagiellonian University, 30–059 Cracow, Poland*
[d] *Physikalisch Technische Bundesanstalt, Berlin, Germany*
[e] *Paul Scherrer Institute (PSI), CH–5232 Villigen-PSI, Switzerland*
[f] *Excellence Cluster 'Universe', Technische Universität München, D–85748 Garching, Germany*
[g] *Physics Departement, University of Virginia, Charlottesville, VA, USA*
[h] *ETH Zürich, CH-8093 Zürich, Switzerland*
[i] *Institut Laue–Langevin, F–38042 Grenoble Cedex, France*
[j] *Department of Physics and Astronomy, University of Sussex, Falmer, Brighton BN1 9QH, United Kingdom*
[k] *Technische Universität München, D–85748 Garching, Germany*
[l] *JINR, 141980 Dubna, Moscow region, Russia*
[m] *University of Fribourg, CH–1700, Fribourg, Switzerland*
[n] *Henryk Niedwodniczański Institute for Nuclear Physics, 31–342 Cracow, Poland*
[o] *Michigan State University, East-Lansing, USA*
[p] *LPSC, Université Joseph Fourier Grenoble 1, CNRS/IN2P3, Institut National Polytechnique de Grenoble 53, F–38026 Grenoble Cedex, France*
[q] *Instituut voor Kern– en Stralingsfysica, Katholieke Universiteit Leuven, B–3001 Leuven, Belgium*
[r] *Institut für Kernchemie, Johannes–Gutenberg–Universität, D–55128 Mainz, Germany*

Abstract

The measurement of the neutron electric dipole moment (nEDM) constrains the contribution of CP-violating terms within both the Standard Model and its extensions. The experiment uses ultracold neutrons (UCN) stored in vacuum at room temperature. This technique provided the last (and best) limit by the RAL/Sussex/ILL collaboration in 2006: $d_{\mathrm{n}} < 2.9 \times 10^{-26}$ e cm (90% C.L.). We aim to improve the experimental sensitivity by a factor of 5 within 2-3 years, using an upgrade of the same apparatus. We will take advantage of the increased ultracold neutron density at the Paul Scherrer Institute (PSI) and of a new concept including both, external magnetometers and a cohabiting magnetometer. In parallel, a next generation apparatus with two UCN storage chambers and an elaborate magnetic field control is being designed aiming to achieve another order of magnitude increase in sensitivity, allowing us to put a limit as tight as $d_{\mathrm{n}} < 5 \times 10^{-28}$ e cm (95% C.L.), if not establishing a finite value.

Keywords: Neutron electric dipole moment, Magnetometry, Ultracold neutrons
PACS: 13.40.EM, 14.20.Dh, 07.55.Ge

1. Introduction

The neutron electric dipole moment is a coupling between the neutron spin and an electric field which breaks both parity P and time reversal T symmetries. Since the experimental discovery of P violation in 1957 [1] and of CP violation in 1964 [2] in weak processes, a non-zero contribution to the neutron electric dipole moment is expected from the weak sector. This contribution is however too small to explain the baryonic asymmetry of the universe, providing a strong indication that new sources of CP violation should exist. Some extensions of the Standard Model, e.g. the electroweak baryogenesis model propose a possible solution for the baryonic asymmetry of the universe together with a super symmetry (SUSY) model for particle physics. The neutron electric dipole moment appears as one of the best ways to test such a kind of models and in a more general view, to quantify the level of CP violation in our universe.

The theoretical context is extremely rich: both cosmological arguments (to explain the baryonic asymmetry of the universe a minimal amount of CP violation is necessary) and fundamental arguments from the particle physics side (like new complex phases in super symmetric models) predict a value of the neutron electric dipole moment in the range $10^{-25} - 10^{-28}$ e cm which has been probed or will be probed in the near future.

Our collaboration [3] envisages a two-step procedure:

- The first step is a measurement of the neutron electric dipole moment using an upgraded version of the RAL/Sussex/ILL spectrometer. This spectrometer, while operated by the RAL/Sussex/ILL collaboration set the last and most stringent limit on the neutron electric dipole moment in 2006: $d_\mathrm{n} < 2.9 \times 10^{-26}$ e cm [4]. At that time the main limiting factor was the low ultracold neutron density available. The new UCN source starting at the Paul Scherrer Institute [5] offers a new opportunity for a more sensitive measurement (typically 5×10^{-27} e cm) with this setup. This step will be discussed in detail in Section 3.
- In parallel, our collaboration is designing a new spectrometer called n2EDM. The expected sensitivity is 5×10^{-28} e cm. The status of this part of the project will be given in Section 4.

2. The concept

Both spectrometers are based on a concept involving the storage of UCN in vacuum at room temperature together with the use of different magnetometers to overcome systematic effects. The neutron electric dipole moment, d_n, is measured via the neutron precession frequency ν_n in the presence of a magnetic field B and an electric field E:

$$h\nu_{\mathrm{n},\uparrow\uparrow/\uparrow\downarrow} = |2\mu_\mathrm{n} B \pm 2d_\mathrm{n} E|\,, \tag{1}$$

where μ_n is the neutron magnetic moment, h the Planck's constant and $\uparrow\uparrow$ (resp. $\uparrow\downarrow$) stands for the relative direction of the magnetic and electric fields (e.g. parallel or anti-parallel). The difference between the neutron precession frequency in the parallel configuration and in the anti-parallel configuration gives us access to the neutron electric dipole moment:

$$\nu_{\mathrm{n},\uparrow\uparrow} - \nu_{\mathrm{n},\uparrow\downarrow} = \frac{2d_\mathrm{n}}{h}(E_{\uparrow\uparrow} + E_{\uparrow\downarrow}) + \frac{2\mu_\mathrm{n}}{h}(B_{\uparrow\uparrow} - B_{\uparrow\downarrow}) \tag{2}$$

with a sensitivity limited by the stability of the magnetic field.

A solution to overcome this limitation was proposed and implemented in 1997 by the RAL/Sussex/ILL collaboration and consists of a co-magnetometer [6]. The principle is to let mercury atoms (^{199}Hg) precess in the neutron precession chamber together with neutrons. One can then form the ratio R of the neutron precession frequency to the mercury precession frequency:

$$R_{\uparrow\uparrow/\uparrow\downarrow} = \frac{\nu_\mathrm{n}}{\nu_\mathrm{Hg}} \approx \left| \frac{\gamma_\mathrm{n}}{\gamma_\mathrm{Hg}} \pm \frac{2E}{h\nu_\mathrm{Hg}} \left(d_\mathrm{n} - \frac{\gamma_\mathrm{n}}{\gamma_\mathrm{Hg}} d_\mathrm{Hg} \right) \right| \tag{3}$$

Email address: Stephanie.Roccia@csnsm.in2p3.fr (S. Roccia)
[1] On leave of absence from INRNE, Sofia, Bulgaria.
[2] On leave from PNPI, St Petersburg, Russia.
[3] Also at University of Zürich, Zürich, Switzerland. Now at University of Washington, Seattle WA, USA.
[4] Now at CSNSM, Université Paris-Sud 11, CNRS/IN2P3, Orsay, France.

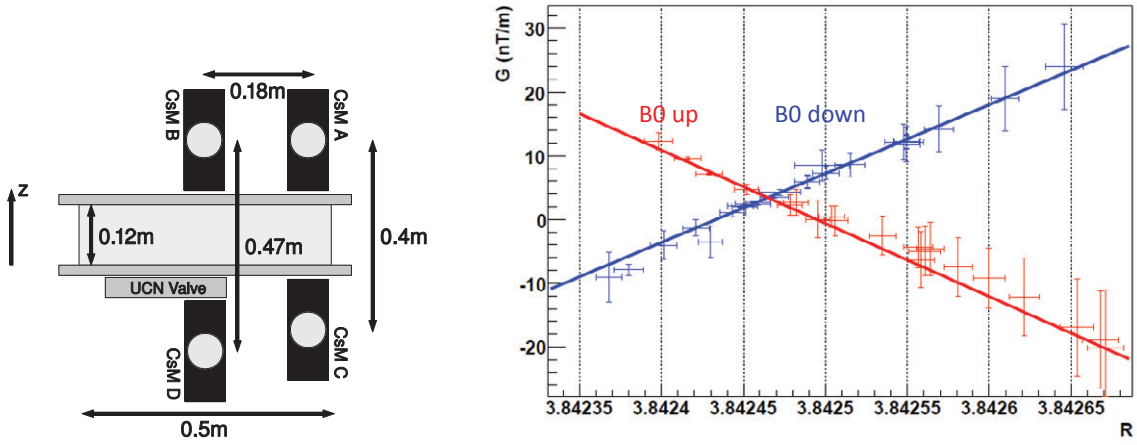

Figure 1: Correlation study between the vertical gradient G and the ratio R of the neutron precession frequency to the mercury precession frequency (see Equation 4). G is the average value of the magnetic gradient measured by pair couple of magnetometers. The left hand scheme shows the position of the four cesium magnetometers during the correlation study. On the right the correlation is shown for both directions of the magnetic field: in red (resp. blue) for the magnetic field pointing upwards (resp. downwards).

where γ_n and γ_{Hg} are the gyromagnetic ratios and only terms linear with the electric dipole moments are considered. The advantage of this observable is that it does not depend on magnetic field fluctuations. The disadvantage is that one measures a combination of both the neutron and the mercury electric dipole moments. But knowing the tight constraint on the mercury electric dipole moment: $d_{Hg} = (0.49 \pm 1.29 \pm 0.79) \times 10^{-29}$ e cm [7], the correction is at the level of 10^{-29} e cm and well under control.

While using this co-magnetometer, the limiting factor is then the vertical gradient of the magnetic field. On the one hand, due to gravity and the low UCN kinetic energy, the UCN density is higher in the lower part of the precession chamber. On the other hand, the mercury density is nearly homogeneous. The different spatial distribution of the two species translates into a different magnetic field average in the presence of a vertical gradient:

$$R_{\uparrow/\downarrow} = \left| \frac{\gamma_n}{\gamma_{Hg}} \left(1 \mp (B/\partial z) \frac{\Delta h}{B} \right) \right| \tag{4}$$

where $\uparrow$ (resp. $\downarrow$) stands for magnetic field up (resp. down) and $\Delta h \approx 2 - 3$ mm is the difference between the centers of mass of the neutrons and mercury atoms.

With the help of cesium magnetometers [8] we have measured the vertical gradients and their fluctuations. This gives us the possibility to increase our sensitivity. Equation 4 was tested in 2008 at the Institut Laue Langevin (ILL) by changing the vertical gradients and studying the effect both on the ratio R and on the vertical gradients measured by four cesium magnetometers. Figure 1 shows the experimental arrangement during this measurement and the result. This study validates the principle of using cesium magnetometers as gradiometers [9].

3. The RAL/Sussex/ILL spectrometer

Figure 2 is a scheme of the upgraded RAL/Sussex/ILL spectrometer as it is now installed at PSI. The neutrons come from the UCN source (from left). They first go through the superconducting magnet where the magnetic field (5 T) is large enough to polarize neutrons at nearly 100 %. The polarized neutrons are then guided to the precession chamber which consists of two electrodes and an insulating ring. Up to this stage, the neutrons are polarized along the magnetic field B_0 (e.g. vertical). Following a radio-frequency pulse tuned in frequency and amplitude, the neutron spins are flipped into the plane perpendicular to the magnetic field and they start precessing. At the end of the precession time, a second pulse equal and in phase with the first one is applied. These two pulses with a free precession interval in-between form the Ramsey procedure of separated oscillating fields and correlate the polarization measured

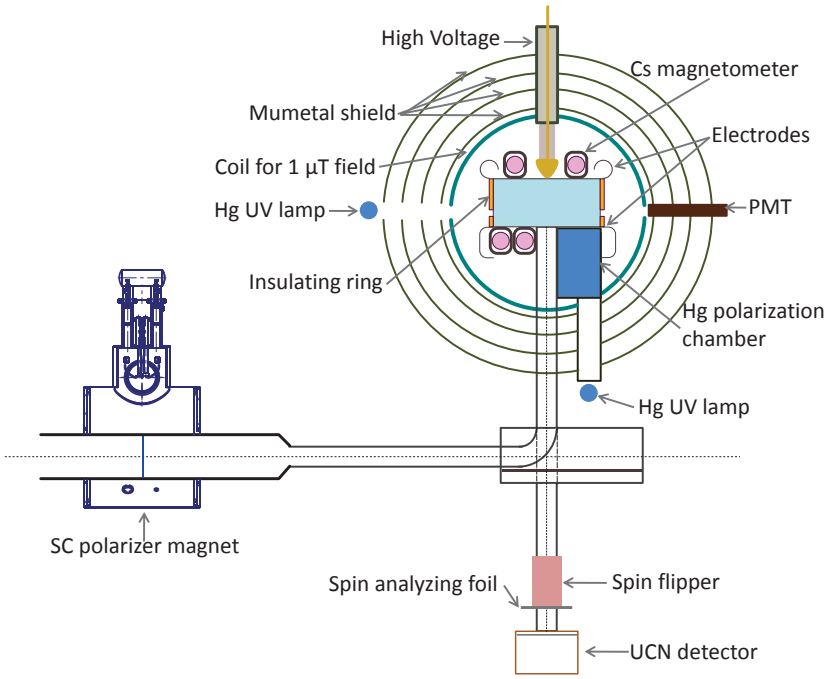

Figure 2: Scheme of renewed RAL/Sussex/ILL apparatus at PSI.

at the very end with the precession frequency and the frequency of both pulses. After this cycle, the shutter of the precession chamber is opened and the neutrons fall down to the detector. With a system including a spin flipper and a polarization analyzer, we can sequentially count the neutrons with spin up and down and thus compute the polarization.

The mercury atoms, needed for the co-magnetometer, are produced from mercury oxide heated to 200 °C and accumulated in the polarization chamber. In this chamber the mercury atom polarization is built up via optical pumping with circularly polarized resonant light. Then the polarized atoms are admitted into the precession chamber with the neutrons and a dedicated radio frequency pulse is applied to flip their spins into the plane perpendicular to the magnetic field. The precession frequency of mercury atoms is probed optically with a resonant polarized light beam going through the chamber. Since the probability of a resonant photon to be absorbed by an atom depends on the relative orientation of the atom spin with respect to the light propagation direction, the transmitted light is modulated at the mercury precession frequency (8 Hz). The 8 Hz signal is filtered and amplified to reach a high signal to noise ratio of 10^3 [6].

3.1. The RAL/Sussex/ILL spectrometer at ILL

For four years (2005-2009), our collaboration operated the RAL/Sussex/ILL spectrometer at the PF2 beamline at the Institut Laue-Langevin. The goal was to recover the best performance of the apparatus and to test new hardware. At the very end of this period, a test measurement of the neutron electric dipole moment was done over an interval of 11 days. We measured a total of 2897 cycles: 1275 with the magnetic field pointing up and 1622 with it pointing down. In both cases, we took data for three different vertical gradients (close to zero, positive and negative). Figure 3 shows the ratio R for all data and the three different magnetic configurations are clearly visible. Because those data were used for many studies, while the magnetic field was pointing upwards, the precession time was changed. As a consequence, and because the UCN storage time is energy-dependant, the UCN spectrum was modified together with the UCN center of mass. This translates into a change of the ratio R (see Equation 4) and the histograms on the right hand side of figure 3 are in fact the sum of a few histograms with a slightly shifted mean value, this explains the bigger

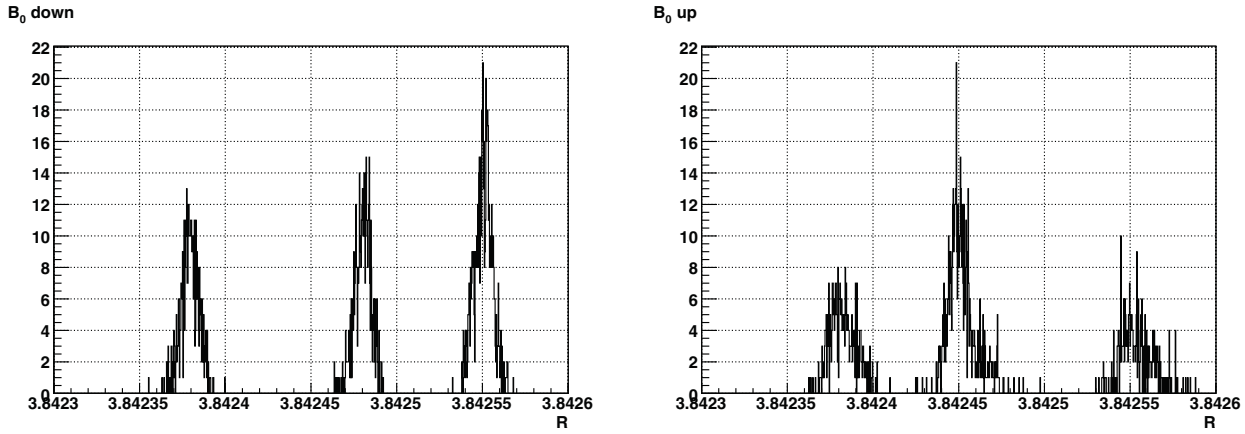

Figure 3: Summary of all data taken to measure the neutron electric dipole moment in 2008 at PF2/ILL. For each direction of the magnetic field (downwards at the left hand side and upwards at the right hand side) 3 magnetic configurations were used with 3 vertical gradients providing 3 different values for the ratio R. The spread around the central value is due to statistical fluctuations and in the B_0 up case, it is enhanced due to modifications of the UCN spectrum (see text for details).

spreads in those histograms. This spread also includes the contribution due to statistical uncertainty. One contribution comes from the uncertainty on the mercury precession frequency ($\sigma_{\nu_{\mathrm{Hg}}}$) [6]:

$$\sigma_{\nu_{\mathrm{Hg}}} = \frac{1}{4T}\frac{a_n}{a_s}\frac{1}{\sqrt{n}}\left(1 + e^{2T/T_{2,\mathrm{Hg}}}\right)^2 = 0.3\,\mu\mathrm{Hz}. \tag{5}$$

where T is the precession time, $\frac{a_n}{a_s}$ is the ratio of noise amplitude to the signal amplitude, n is the number of samples taken on the sine curve and $T_{2,\mathrm{Hg}}$ is the mercury transverse depolarization time defining the decay time of the amplitude of the signal. But the main contribution comes from the uncertainty of the neutron precession frequency ($\sigma_{\nu_{\mathrm{n}}}$):

$$\sigma_{\nu_{\mathrm{n}}} = \frac{1}{2\pi T\alpha\sqrt{N}} \tag{6}$$

where N is the number of neutrons and $\alpha = \alpha_0 e^{-T/T_{2,\mathrm{n}}}$ is the visibility parameter which depends mainly on the neutron polarization after its rotation in the horizontal plane. The time dependence of the visibility α depends on the relaxation time $T_{2,\mathrm{n}}$ of the neutron polarization during a free precession process. We had $\alpha_0 = 0.86 \pm 0.01$ and most of the data were taken with $T = 130$ s where typically $N = 4600$. For the best magnetic settings we observed $T_{2,\mathrm{n}} = (400 \pm 38)$ s and thus,

$$\sigma_{\nu_{\mathrm{n}}} = 30\,\mu\mathrm{Hz}. \tag{7}$$

The first step in the analysis is to fit the neutron count rate for both spin up and down to the Ramsey curve to extract the neutron precession frequency [6]. At this stage only one cut is applied: count rates which deviate by more than 4 standard deviations from the curve are excluded. This affects 6 % of the data.

The last step is the extraction of the neutron electric dipole moment. A linear dependence between the ratio R and the electric field is sought. A different fit is done for each magnetic configuration and each storage time, see figure 4. The results are then combined independently for each direction of the magnetic field and lead to:

$$\text{For } B_0 \text{ down} \quad d_{\mathrm{n}} = (-3.7 \pm 2.2) \times 10^{-25}\ e\ \mathrm{cm}\ (\chi^2 = 7/10) \tag{8}$$

$$\text{For } B_0 \text{ up} \quad d_{\mathrm{n}} = (7.3 \pm 3.9) \times 10^{-25}\ e\ \mathrm{cm}\ (\chi^2 = 7/2) \tag{9}$$

One can also combine all data together which gives:

$$d_{\mathrm{n}} = (-1.0 \pm 1.9) \times 10^{-25}\ e\ \mathrm{cm}\ (\chi^2 = 21/13). \tag{10}$$

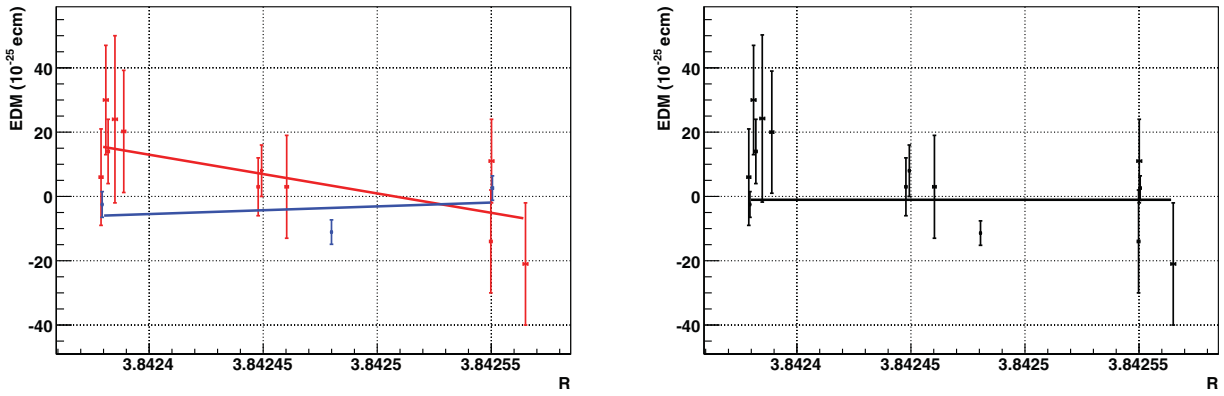

Figure 4: Dependence of the neutron electric dipole moment on the ratio R. On the left hand side, the study is done independently for the two directions of the magnetic field: in blue for B_0 down and in red for B_0 up. On the right hand side, the study is done for all data together and the combined value is extracted.

The expected statistical precision was 1.6×10^{-25} e cm (20 % smaller than the 1.9×10^{-25} e cm measured) assuming that all data are taken in the best magnetic configuration and with the optimal (130 s) precession time which was not the case. However, the number proves that our system was performing well.

When using the co-magnetometer, one limiting factor is a systematic effect sometimes referred to as the geometrical phase effect which has been observed and studied previously [10] with the same apparatus. This effect is a Ramsey-Bloch-Siegert shift of the precession frequency of confined spins which is proportional to the electric field and thus mimics an electric dipole moment signal. Due to the high (at least high in comparison with UCN) average mercury velocity, this effect is bigger for the mercury atoms. Additionally, this shift is proportional to the magnetic vertical gradient meaning that we can make a measurement of the neutron electric dipole moment free from this effect if the magnetic configuration is such that: $\partial B/\partial z = 0$.

One can also employ larger vertical gradients to see this effect and interpolate to correct for it. This was the solution chosen in [4]. Then a linear correlation between the ratio R and the measured electric dipole moment should appear since they both depend linearly on the vertical magnetic gradients. Furthermore, the linear dependence between R and $d_{\mathrm{n,\ meas}}$ is expected to be the same but with an opposite sign for each direction of the magnetic field due to the $1/B$ dependence in equation 4.

Despite expecting insufficient statistics, we tried to isolate this effect in the December 2008 data set. There we worked at 3 different vertical magnetic gradients for each direction of the magnetic field, see the left panel of figure 4. A slope p could be extracted for each direction of the magnetic field:

$$\text{For } B_0 \text{ down} \quad p = (2.2 \pm 3.2) \times 10^{-21}\ e \text{ cm } (\chi^2 = 6/1) \tag{11}$$

$$\text{For } B_0 \text{ up} \quad p = (-12.1 \pm 6.5) \times 10^{-21}\ e \text{ cm } (\chi^2 = 4/9) \tag{12}$$

If one assumes a common slope, this yields:

$$p = \pm(7.2 \pm 3.6) \times 10^{-21}\ e \text{ cm} \tag{13}$$

where + (resp. −) stands for the magnetic field pointing downwards (resp. upwards). This result is in agreement with the expected value [4]:

$$p_{\mathrm{theo}} = \pm(4.1 \pm 0.2) \times 10^{-21}\ e \text{ cm}. \tag{14}$$

3.2. The RAL/Sussex/ILL spectrometer at PSI

From equation 6 one can derive the statistical uncertainty of the measurement of the neutron electric dipole moment:

$$\sigma_{d_{\mathrm{n}}} = \frac{\hbar}{2\alpha E T \sqrt{N}}. \tag{15}$$

In the following section, we will discuss efforts made to improve this accuracy.

The visibility α

The visibility, α, depends not only on the initial polarization but also on $T_{2,n}$. With our newly installed superconducting magnet, the initial polarization can be close to 100 % and will be probably limited by the quality of the polarization transfer through the shield. We also work to reduce the depolarization during the precession time which is dominated by magnetic inhomogeneities. To reduce those inhomogeneities, we have, in addition to the main coil, installed a set of 33 trim coils with different geometries and independent power supplies. Magnetic maps have been recorded of each of those coils and the 33 optimized currents have been deduced. The optimized magnetic configuration itself has been mapped and shows no transverse component bigger than half a nanotesla and a maximum gradient of 4 nT/m. Also, due to a new degaussing system, the magnetic field is reproducible at a level better than the sensitivity of the flux gates of 0.5 nT.

We expect $\alpha = 0.75$ after a precession time of 150 s with $\alpha_0 = 0.95$ and $T_{2,n} = 600$ s.

The precession time T

We foresee to work at precession times of typically 150 s. This is possible using a new insulator for the precession chamber made from polystyrene and coated with deutered polystyrene (dPS). It provides a higher material optical potential (161 neV) [11] than quartz (90 neV) and thus the possibility to store neutrons with velocities less than 5.5 m/s as compared to quartz, where neutrons could be stored with velocities $v < 4.2$ m/s only. After a storage time of 150 s, we had 1.8 times more neutrons in the dPS chamber as in the previous quartz chamber [11].

In order to increase the precession time together with decreasing the systematic effects, one needs to increase the temporal stability of the magnetic field and magnetic field gradients. The major source of fluctuations of the magnetic field is related to the magnetic shield and, in particular, to the rearrangement of magnetic domains. To reduce this effect, the shield has been put in a thermally insulated room and it is standing on a support which strongly suppresses ambient vibrations. A new degaussing system together with a new degaussing procedure shows a reduction by factor 10 of the field changes created artificially, e.g by mechanical shocks on the shield support. The second source of magnetic fluctuations is due to the fluctuations of the magnetic field outside the shield. To reduce this effect, an active magnetic shield has been installed: six 6×8 m^2 rectangular coils produce a magnetic field to actively compensate ambiant magnetic field by means of a feedback loop controlled by flux gate magnetometers. We achieved in the best case a suppresion of the magnetic fluctuations inside the mu-metal shield by a factor of 10 but in average a suppression factor of 2 was observed. Further improvement may be possible.

The electric field E

A new bipolar high voltage supply (±200 kV) together with a newly designed HV feed through will in principle allow us to increase the electric field strength. However, the performance of the co-magnetometer had always limited the electric field strength to 130 kV and so far, we do not expect that this can be overcome.

The number of neutrons N

We expect a 25-times higher UCN density in our apparatus from the new PSI source. While the increase in the source strength should be even more, the present setup cannot yet make full use of it because it is not optimally adapted to the energy spectrum provided by the source. We expect for our new measurement scheme rates of detected UCN up to 10^6 s^{-1}. This has previously been beyond the capability of conventional single channel UCN detectors. A segmented system of detection with nine sections based on ^{6}Li doped glass scintillators has been developed. Each of the sections is a two-layer stack composed of a ^{6}Li-depleted scintillator (GS30, thickness: 60 μm) fused to a ^{6}Li-enriched (GS20, thickness 120 μm) scintillator. The former has a low UCN absorption probability (around 5 %) while the latter one has essentially 100 % absorption probability. Within such a scintillator, the neutron detection is performed with the ^{6}Li neutron capture reaction: n + ^{6}Li $\rightarrow$ ^{3}H (2.74 MeV) + ^{4}He (2.05 MeV) [12]. The advantage of the layer construction is that most of the decay products from the neutron capture reaction can be contained within the scintillator stack if the thickness of the first layer exceeds the range of the decay products. As a result, all the energy released by the neutron capture is collected, which improves the separation between the neutrons and the gamma contributions. This is clearly seen in the panels 1 to 8 of the figure 5 for which the background discrimination is good.

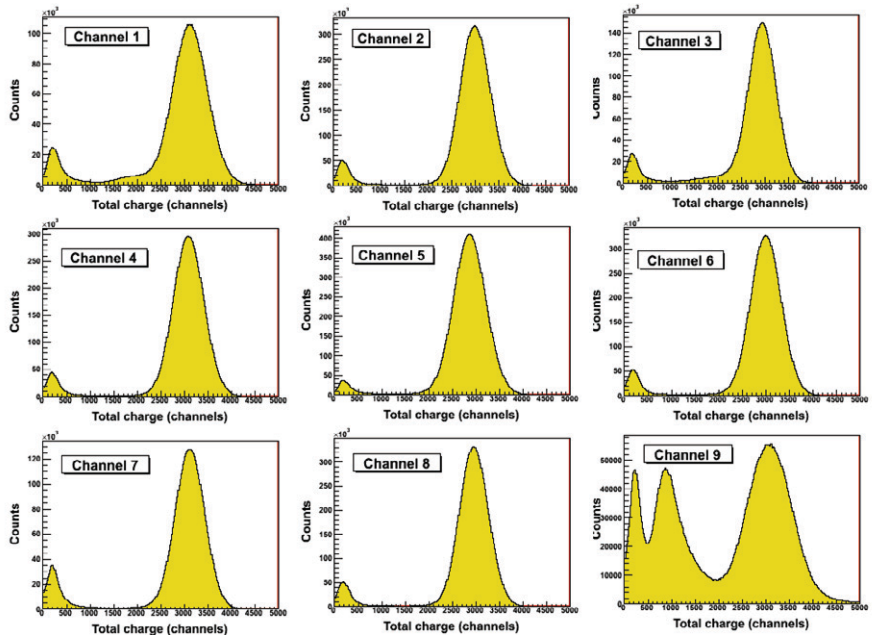

Figure 5: UCN spectra recorded at the PF2/ILL with the new segmented two-layer glass scintillator stack detector. For demonstration, the last panel corresponds to the segment equipped with a single scintillator.

In panel 9, a single ^{6}Li enriched scintillator has been used: for a fraction of the detected neutrons, one of the decay products escapes from the glass resulting in a poor separation between the neutron peak and the background.

After taking into account all the upgrades and improvements the statistical uncertainty is expected to be:

$$\sigma_{d_{\mathrm{n,PSI}}} = 4 \times 10^{-25}\ e \text{ cm per cycle} \quad (16)$$

$$\sigma_{d_{\mathrm{n,PSI}}} = 3 \times 10^{-27}\ e \text{ cm per year} \quad (17)$$

assuming data taking only during nights and systematic studies during day time. Then our sensitivity goal will be achieved after two years.

4. n2EDM

In parallel, our collaboration is working on a new spectrometer with the idea to push the ”room temperature in vacuum” concept as far as possible. Figure 6 shows a sketch of the current concept. The geometry of the magnetic shield (see figure 6 on the left) has been defined based on two requirements: a high shielding factor (typically 10^5 for frequencies between 0 and 100 Hz) together with a good magnetic field homogeneity (all gradients smaller than 1 nT/m). The high magnetic shielding factor can be achieved with a 4 layer cubic mu-metal shield. The performances of such shields have been proven and this geometry offers good technical solutions to open and close the shield. On the other hand, the magnetic field is deformed due to the corners. Since the magnetic homogeneity is mainly due to the innermost magnetic shield layer we chose a cylindrical geometry for the innermost layer.

On the right hand side of figure 6 the concept of the chambers is presented. The two precession chambers are one above the other and separated by the high voltage electrode. This provides an opposite electric field in each chamber while they are in the same magnetic field. With this geometry both configurations ($\uparrow\uparrow$ and $\uparrow\downarrow$) in Equation 2 are measured at the same time, providing a better control of systematic effects.

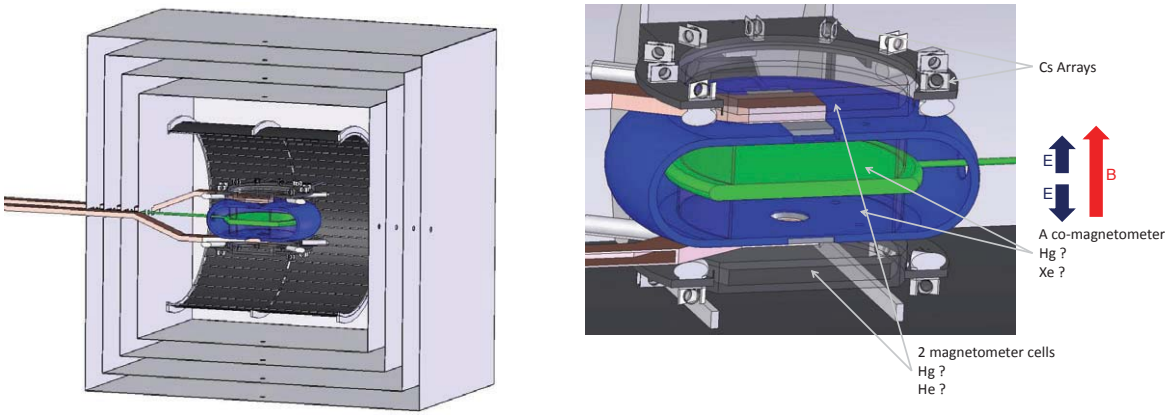

Figure 6: Schemes of the n2EDM spectrometer. On the left hand side, a cut of the system except for the superconducting magnet. On the right hand side, a zoom on the two big neutrons precession chambers and on the magnetometry system.

We plan to use a co-magnetometer and currently we are studying two promising candidates: ^{199}Hg and ^{129}Xe. It will be used to investigate the possible differences between the magnetic fields in the two chambers. We are also developing solutions for the two magnetometer chambers investigating in parallel ^{199}Hg and ^{3}He. The advantage of such a couple of big chambers is that it gives access to the incoming and outgoing magnetic flux and thus to magnetic field gradients over the neutron chambers. This information, together with the co-magnetometer information will be an important tool to, e.g., correct for geometrical phase effects. In addition, external magnetometers will be used as gradiometers and to read out the modulated magnetization signal from the ^{3}He magnetometers.

5. Conclusion

Our collaboration is now ready for data taking at PSI with the upgraded apparatus. With the new UCN source at PSI and the performances demonstrated during the tests in 2009/2010 we should be able to achieve a statistical acuracy of $\sigma_{d_{\mathrm{n,PSI}}} = 3 \times 10^{-27}$ e cm per year. The control of systematic effects will be also improved, in particular by the use of Cs magnetometers used as gradiometers. It will take about two years to reach a sensitivity of $d_{\mathrm{n}} < 5 \times 10^{-27}$ e cm (95% C.L.).

References

[1] C. S. Wu, E. Ambler, R. W. Hayward, D. D. Hoppes and R. P. Hudson: Phys. Rev. **105**, 1413 (1957).
[2] J. H. Christenson, J. W. Cronin, V. L. Fitch and R. Turlay: Phys. Rev. Lett. **13**, 138 (1964).
[3] https://nedm.web.psi.ch/
[4] C. A. Baker *et al.*: Phys. Rev. Lett. **97**, 131801 (2006).
[5] A. Anghel *et al.*: Nucl. Instrum. Methods Phys. Res., Sect. **A 611**, 272-275 (2009).
[6] K. Green *et al.*: Nucl. Instrum. Methods Phys. Res. , Sect. **A 404**, 381 (1997).
[7] W. C. Griffith *et al.*: Phys. Rev. Lett. **102**, 101601 (2009).
[8] S. Groeger, A. S. Pazgalev, A. Weis: Appl. Phys **B 80**, 6 (2005).
[9] S. Roccia: PhD thesis, Université Joseph Fourrier, Grenoble (2009).
[10] J. M. Pendlebury *et al.*: Phys. Rev. **A 70**, 032102 (2004).
[11] K. Bodek *et al.*: Nucl. Instrum. Methods Phys. Res., Sect. **A 597**, 222-226 (2008).
[12] G. Ban *et al.*: Nucl. Instrum. Methods Phys. Res., Sect. **A 611**, 272 (2009).